Frequency generation within the forbidden band gap: All optical Rabi-like splitting in photonic crystals and microcavities

Claudio Conti,* Andrea Di Falco, and Gaetano Assanto
NooEL, Nonlinear Optics and OptoElectronics Laboratory, National Institute for the Physics of Matter, University Roma Tre, Via della Vasca Navale, 84-00146 Rome, Italy

(Received 27 April 2004; revised manuscript received 3 August 2004; published 15 December 2004)

Based on three-dimensional time domain numerical simulations of the nonlinear dispersive Maxwell equations, we find evidence of all optical splitting of defect states in a photonic band gap structure. The result is analogous to the well known Rabi splitting and optical nutation in atomic two-level systems, and can be used for controlled in-gap generation of optical frequencies. Photon-echo-like behavior and third harmonic generation are also investigated.

DOI: 10.1103/PhysRevE.70.066614 PACS number(s): 42.70.Qs, 02.70.Bf, 42.65.Yj, 78.47.+p

Photonic crystals (PC's) and nanostructured dielectric periodic media can exhibit photonic band gaps (PBG's), i.e., frequency regions where no states are available to propagation of electromagnetic (EM) radiation [1,2]. This property of PC's was originally singled out and suggested by Yablonovitch for improving the efficiency of photonic devices, and by John for light localization [3,4].

PC structures, spatially extending for only a few wavelengths, afford a dramatic redistribution of EM states. In doing so, while providing the grounds for a new generation of highly integrated optical circuits, they also encompass a wealth of fundamental EM phenomena in modern physics. Stemming from the seminal work by Purcell [5], the inhibition of emission processes in the absence of available states for EM radiation is the foundation, among other things, of highly efficient solid-state lasers [3]. In analogy to the linear case, inhibition has been considered to hold for nonlinear emission or amplification processes such as frequency doubling or parametric generation in the photonic band gap [1].

Conversely, it is well understood that a nonlinear refractive response at high fluencies can alter the photonic band structure [6,7], leading to various intriguing phenomena (recently reviewed in [8,9]). Some preliminary experimental investigations to this extent have been reported [10,11]. In addition, high Q factors in resonators can significantly lower the power threshold in nonlinear processes, and favor further achievements in microcavities [12,13].

In this article we demonstrate that photonic band gaps are not actually "forbidden," i.e., at variance with what is expected on linear grounds, nonlinear optical processes can efficiently generate frequencies well within these energy intervals. This work, originating from investigations on photonic crystal spectroscopy by ultrafast optical nonlinearity, relates also to the recent achievements in transient material spectroscopy (see, e.g., [14]). We predict hereby the existence of an optical phenomenon resembling Rabi oscillations, i.e., the interaction-driven splitting of a resonant level. Such effect in an optical PBG could enable all optical control of in-gap frequency generation in PC's and microcavities, where the nonlinear optical susceptibility can play the role of an external electric field applied to a two-level system. The splitting is apparent when considering the spectra of the generated third harmonic, as well. We also point out remarkable analogies with other processes from ultrafast spectroscopy, namely, optical nutation and photon echo.

The starting point of our analysis is the *ab initio* numerical solution of nonlinear three-dimensional (3D) Maxwell equations in the time domain. Since the coupling of cavity to radiation modes through finite Q factors is at the basis of relaxation phenomena, such an approach is mandatory. The geometry we consider here is the simplest 3D high-index-contrast structure exhibiting a PBG: the photonic crystal wire (PCW) [15,16]. While the analysis can be applied/extended to any microcavity or PC in isotropic nonlinear media, the chosen configuration enables the simple control of cavity parameters, such as lifetime and resonant frequency. The PCW 3D device is periodic in one dimension, with a single defect in its repeated cell with high index contrast (see Fig. 1), thus providing high EM field concentration in a few micrometers length.

We integrated the nonlinear Maxwell equations cast in the form

$$\nabla \times \mathbf{E} = -\mu_0 \partial_t \mathbf{H}, \quad \nabla \times \mathbf{H} = \epsilon_0 \partial_t \mathbf{E} + \partial_t \mathbf{P},$$

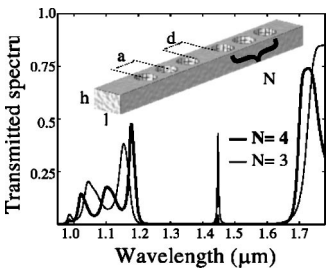

FIG. 1. Transmitted spectrum of the photonic crystal wire with a defect cavity, as sketched in the inset, for two different number of holes on each side.

*Electronic address: c.conti@ele.uniroma3.it
URL: http://optow.ele.uniroma3.it/opto_2002.shtml

$$\partial_t^2 \mathbf{P} + 2\gamma_0 \partial_t \mathbf{P} + \omega_0^2 f(P)\mathbf{P} = \epsilon_0(\epsilon_s - 1)\hat{\omega}_0^2 \mathbf{E}, \qquad (1)$$

where $f(P)$ describes the nonlinear response of the material. $f(P)=1$ corresponds to a linear single-pole Lorentz dispersion relation with resonant (angular) frequency ω_0, loss coefficient γ_0, and static dielectric permittivity ϵ_S. $f(P)=[1+(P/P_0)^2]^{-3/2}$, with $P^2=\mathbf{P}\cdot\mathbf{P}$, retrieves a simple Kerr response for small P [17], whereas for larger P it accounts for higher-order nonlinear terms (e.g., $\chi^{(5)}$ and saturation). Compared to alternative formulations in nonlinear finite difference time domain (FDTD) codes [18], the simple nonlinear oscillator above is an appropriate model for ultrafast (but not reduced to instantaneous) electronic nonlinearities [19], and enables us to include the relevant physics while neglecting Raman and carrier injection processes.

To draw attention to a specific material of current technological interest, we adopted parameters which fit the linear dispersion relation of $Al_xGa_{1-x}As$ (refractive index $n \cong 3.5$ at $\lambda = 1.55$ μm) in the frequency region of interest [20]. Note, however, that similar values apply to other semiconductors with comparable refractive index and nonlinear response, such as silicon [21]. The details of the algorithm, based on the approach developed for linear media in [22] and on an FDTD scheme [18] will be reported elsewhere.

The defect in the PCW is placed in the middle of the device (Fig. 1, inset). The width and wavelength position of the resonance depend on the overall number of holes, which affect both the Q factor Q_0 due to radiation losses and the Q factor responsible for the coupled waveguides Q_e [15]. The latter (with transverse dimensions $h=270$ nm and $l=450$ nm; see Fig. 1) support only the lowest-order TE-like guided mode in the spectral region under consideration; one of them can feed the PCW cavity.

The PCW transmission spectrum can be determined through time domain analysis, so that both the dispersion and the finiteness of the structure (including coupling and radiation losses) are taken into account. A broadband pulse is launched and travels via the input waveguide into the PCW: then the signal spectrum at the output guide is acquired and analyzed. The resulting transmission is graphed in Fig. 1 for two PCW's with different numbers N of holes on each side (see inset), but designed to exhibit nearly the same resonant frequency ω_0 for the defect state ($a=450$ nm, $d=0.75a$, for both $N=3$ and 4). A photonic band gap with an inner defect state is apparent in both curves.

The responses in Fig. 1 were obtained at low input peak power ($P_{in}=1$ nW). To investigate the PCW nonlinear operation, we considered a quasi-cw excitation and higher P_{in}. Since particular care is necessary to avoid steep gradients in the input wave form, we numerically mimicked a quasi-cw wave form with a smooth transition from zero to the peak P_{in}. Such input (an "mnm" pulse) has a narrow bandwidth, introduces no spurious artifacts, and provides quasi-cw pulses [23].

Figure 2 shows the output signal spectrum for three different excitations and a PCW with $N=4$. The input wavelength corresponds to the defect state (see Fig. 1). At high fluencies the formation of sidebands is clearly visible around the resonance and well inside the PBG. Their positions vary

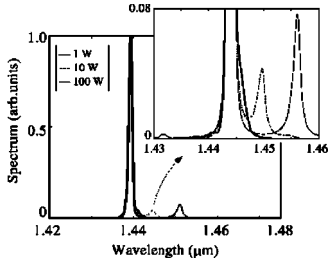

FIG. 2. Output spectrum for various input powers and a PCW with $N=4$. The inset is an enlargement around the defect resonance.

with excitation as in Fig. 3(a), displaying the frequency shift of the lobes versus injected power. The cubic (Kerr-like) nonlinearity mediates the generation of frequencies within the "forbidden" PBG.

In order to provide a theoretical framework to the analysis above, we applied the time domain coupled mode theory [24,25]. The evolution equations for the defect mode can be cast in terms of a normalized amplitude a as

$$\frac{da}{dt} = -i\omega_0 a + i\omega_0 g|a|^2 a - \frac{a}{\tau} + \sqrt{\frac{2}{\tau_e}} s_+ e^{-i\omega t}, \qquad (2)$$

with τ the overall decay constant including radiation, material, and coupling losses, and τ_e the decay constant owing only to the coupling with the feeding waveguide. $|a|^2$ is the energy stored in the defect mode at time t, $P_{in}=|s_+|^2$, with s_+ the amplitude of the feeding guided mode of frequency ω. g is the real-valued three-dimensional overlap integral between the vectorial defect mode profile and the distribution of the $\chi^{(3)}$ response (nonlinear terms containing derivatives of a and higher order nonlinearities are neglected). *Loaded* and *external* Q factors are $Q=\omega_0\tau/2$ and $Q_e=\omega_0\tau_e/2$, respectively.

To inquire into the origin of the generated sidebands, we performed a perturbative analysis with respect to the stationary solution $a=a_0\exp(-i\omega t)$, given by (s_+ can be taken real valued without loss of generality, and $\Delta=\omega-\omega_0$)

$$i\Delta a_0 + i\omega_0 g|a_0|^2 a_0 - \frac{a_0}{\tau} + \sqrt{\frac{2}{\tau_e}} s_+ = 0. \qquad (3)$$

Writing $a=(a_0+a_1)\exp(-i\omega t)$, at the lowest order in a_1 we find

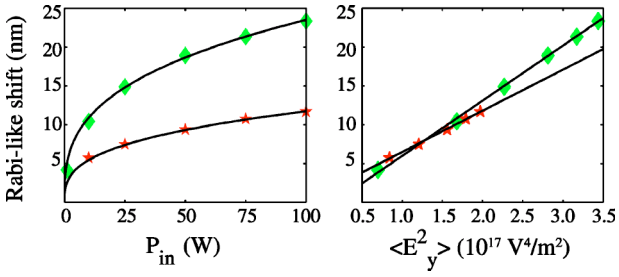

FIG. 3. (Left) Frequency shift of the generated sidelobe inside the PBG (see Fig. 2) vs input power: stars ($N=4$) and diamonds ($N=3$) are computed points, lines are derived from the theoretical model; (right) generated frequency shift versus average squared electric field in the cavity.

$$\dot{a}_1 = i\Delta a_1 - \frac{a_1}{\tau} + i\omega_0 g(2|a_0|^2 a_1 + a_0^2 a_1^*). \tag{4}$$

Equation (4) can be rewritten in terms of $w=|a_1|^2$, $p=a_1^2$, $E=a_0^2$, obtaining

$$\frac{dw}{dt} = -\frac{w}{T} + ig\omega_0(Ep^* - pE^*),$$

$$\frac{dp}{dt} = \left(i\Delta' - \frac{1}{T}\right)p + 2ig\omega_0 Ew, \tag{5}$$

with $T=\tau/2$ the energy decay rate of the cavity mode. Equations (5) are formally identical to those describing an atomic two-level system in the presence of an electric field [19], which in our case corresponds to the squared amplitude $E=a_0^2$, whose modulus is denoted hereafter by $\mathcal{E}_0=|E|=|a_0|^2$ (we use the symbol E to stress the correspondence with the resonant atom density matrix equations, where E typically denotes the applied electric field). For the atomic system, w is the difference between the diagonal elements of the density matrix, p the off-diagonal element, and $\Delta'=2\Delta+4g\omega_0\mathcal{E}_0$ the detuning from resonance. In the PC, the latter also includes the shift due to the Kerr effect.

By reducing the temporal dynamics of our microresonant (PC) system to a well-known model, we have established a relevant connection with the theory of laser-matter interactions. For a cavity with an infinite lifetime, e.g., in the absence of relaxation ($1/T\rightarrow 0$, corresponding to an infinitely large Q factor), the model (5) predicts a splitting of the two-level system (defect mode) resonance into two levels, their separation being proportional to the magnitude of the electric field (to the energy stored in the cavity) $|E|$ in the laser-field interaction (in the PCW). The new PCW levels are $\omega_\pm=\omega_0\pm\mu$, with Rabi-like splitting $\mu=\sqrt{(\Delta'/2)^2-g^2\omega_0^2\mathcal{E}_0^2}$. At exact matching between pump and resonant mode frequency ($\Delta=0$), it is $\mu=\sqrt{3}\omega_0|g|\mathcal{E}_0$. Figure 3(b) shows the frequency shift versus the average electric field E_y squared (proportional to the stored energy $\mathcal{E}_0$) in a low-symmetry point inside the defect cavity. A linear dependence is visible, with no significant difference between the cases $N=3$ and 4. In fact, the modes have frequencies close to the PBG center, hence they rapidly decay along the waveguide and the g coefficient (which provides the slope) is nearly the same.

From a physical point of view, the new states correspond to the defect mode oscillating at two new frequencies, thus strongly resembling a two-level atomic system [19]. In some sense the nonlinear susceptibility "dresses" the defect state by creating additional levels, which can be probed by small signals superimposed to the pump beam, as will be reported elsewhere. This Rabi-like feature of a PC microcavity points out the possibility of all optical tunable emission at frequencies inside a photonic band gap. In Fig. 3 the frequency shift is plotted vs two different quantities, the input power and the average squared electric field, which is proportional to the energy stored in the cavity. To determine a functional relationship between the latter, hence the explicit power dependence of the generated frequency shift proportional to $\mathcal{E}_0$, Eq. (3) needs be solved for a_0. For $\Delta=0$ (as in the numerics) Eq. (3) leads to

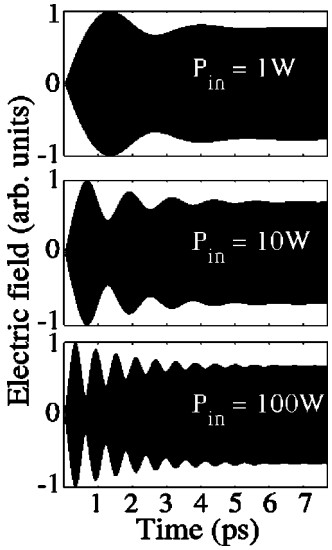

FIG. 4. Electric field E_y in the cavity for various input powers ($N=4$).

$$u^3 + u - w = 0 \tag{6}$$

with normalized energy $u=\omega_0\tau g\mathcal{E}_0$ and power $w=2\omega_0 g\tau^3 P_{in}/\tau_e$. Solid lines in Fig. 3(a) are obtained after Eq. (6) and exhibit the correct trend. By varying the number of holes, because of the highly localized nature of the defect modes, only the (coupling) factor Q_e is affected, while the (radiation loss) factor Q_0 remains nearly the same in both PCW's. The different frequency shifts attained for $N=3$ and 4 can therefore be explained by referring to variations in Q_e, higher in the four-hole PCW because of a more isolated cavity. Roughly, for large $\mathcal{E}_0$ it is $u\cong w^{1/3}$ from Eq. (6), corresponding to $\mathcal{E}_0\propto(P_{in}/Q_e)^{1/3}$ and linking higher Q_e to smaller shifts.

The asymmetric peak in Fig. 2 can be explained by recalling that if a high Q cavity is excited out of resonance, the transient signal spectrum contains input and resonance frequencies, the latter decaying with the cavity lifetime [25]. When including the Kerr effect, such beating is present even for resonant pumping ($\Delta=0$, as in the present case). In fact,

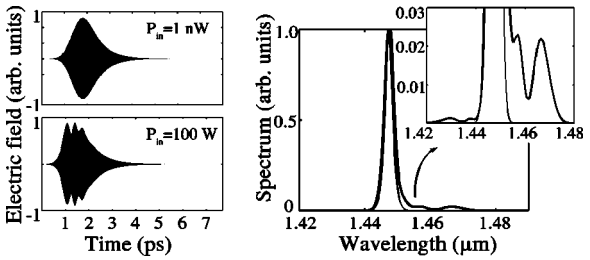

FIG. 5. Temporal response with 0.5 ps input pulses in the case $N=4$. (Left top) low power and (left bottom) high power excitations; (right) corresponding output spectra (thick and thin lines for high and low powers, respectively).

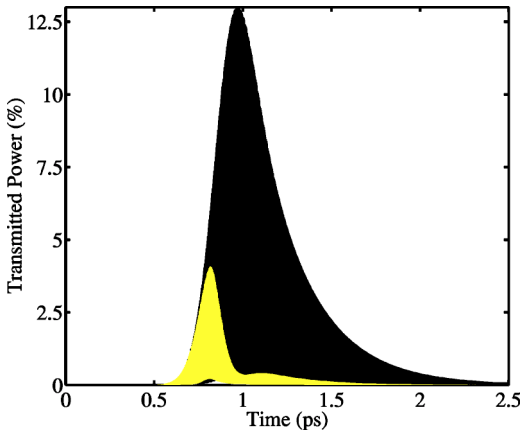

FIG. 6. (Color online) Fraction of transmitted power, for two different input peal powers (10 W dark region, 100 W bright region) for 200 fs input pules. The input wavelength corresponds to the defect state (1447 nm).

the mode frequency is redshifted because of the power dependent refractive index and, during the initial transient, most of the input energy transfers to the shifted mode $\omega_0 - \mu$. Then, through four-wave mixing, $\omega_0 + \mu$ is generated as well, albeit with a lower amplitude of its corresponding peak. Such a result is found here for both the reduced model Eq. (2), not shown, and the whole set of nonlinear Maxwell equations (1).

In perfect analogy with the theory of Rabi oscillations, if relaxation phenomena (e.g., a finite lifetime) are included in the model, they are expected to damp out in time [19]. This is straightforward from both Eq. (5) with $1/T > 0$ and the numerical results, if simulations are carried out for much longer than the energy decay time of the cavity mode. To enlighten this process while limiting computation times, we designed the PCW cavity for a lifetime of the order of 1 ps. Figure 4 displays the temporal evolution of the electric field at a low-symmetry point in the cavity and for a steplike excitation, revealing the progressively damped all-optical Rabi-like oscillations corresponding to the *optical nutation* [26,27]. Strikingly, a classic phenomenon in laser-matter interaction clearly has an all optical counterpart in nonlinear optical microcavities or PC's. Since the generated frequency has the lifetime of the cavity mode (when $\Delta = 0$), for high Q factors the (Rabi-like) frequency splitting could be observed with pulses of durations typically employed in nonlinear optics. We repeated the simulations using 0.5 ps input Gaussian pulses, at high peak powers the in-gap frequency generation was visible in the output signal spectrum, as shown in Fig. 5. There is a strong analogy with transient nonlinear spectroscopy when considering the excitation of resonant systems and metastable states with transient times much shorter than the lifetime [28].

The cavity response to shorter pulses is remarkable (see Fig. 6 where $N = 3$). At low powers the system behaves as a Lorentzian filter, and because of the high Q, the output pulse

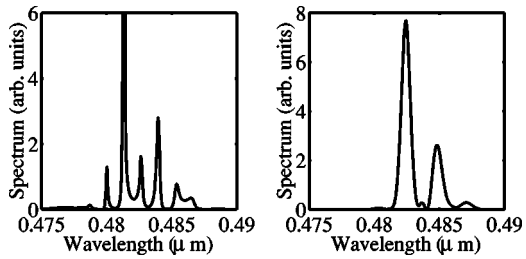

FIG. 7. Output spectrum around the third harmonics of the pump beam for quasi-cw (left) and Gaussian (right) excitations ($P = 100$ W, $N = 4$).

is much longer than the input, with durations of the order of the cavity lifetime. Conversely, at high powers the output full width at half maximum is drastically narrowed. The transmitted pulse at high power contains a small and shorter portion of the input compared to the quasilinear case, with a distorted asymmetric shape and a faster decay. This can be understood through the creation of additional complex poles (the transient modes) that widen the system passband and permit faster responses. The appearance of an additional, delayed, and widened satellite pulse can be intuitively described as the all optical counterpart of the so-called photon echo [29]. While at first glance such an effect could suggest applications in signal regenerators, the drastic reduction of transmission due to the resonance shift tends to hamper such a use and calls for further investigations, which will be reported elsewhere.

The high-power dynamics discussed in Figs. 4–6 can be summarized as follows: for a cw excitation the system settles to a cw output state after sufficiently long times, eventually showing some oscillations due to complex poles, or metastable states. For long pulses, in proximity of their peak, the system response resembles the cw behavior. For short pulses, the cavity is not able to follow very fast excitations, and the response exhibits satellite pulses following the input one (see Fig. 6).

It is noteworthy that, due to the resonant nature of this system, even the generated third harmonic exhibits side peaks which, however, lie outside the photonic band gap. In Fig. 7 the output spectra obtained for quasi-cw and pulsed excitations show the appearance of replicated split frequencies due to various four-wave mixing interactions.

In conclusion, using an *ab initio* approach and including three spatial dimensions and time, we have shown that in high-Q-factor microcavities, here realized by a defect in photonic crystal wires of cubic semiconductors, all optical Rabi-like splitting, optical nutation, and photon-echo-like behaviors can be observed. Such effects could be exploited in the generation of all optically tuned frequencies well inside a photonic band gap.

We acknowledge support from INFM "Initiative Parallel Computing," the Tronchetti Provera Foundation, and the Italian Electronic and Electrical Engineering Association (AEI).

[1] K. Sakoda, *Optical Properties of Photonic Crystals* (Springer-Verlag, Berlin, 2001).
[2] J. D. Joannopoulos, P. R. Villeneuve, and S. Fan, *Photonic Crystals* (Princeton University Press, Princeton, NJ, 1995).
[3] E. Yablonovitch, Phys. Rev. Lett. **58**, 2059 (1987).
[4] S. John, Phys. Rev. Lett. **58**, 2486 (1987).
[5] E. M. Purcell, Phys. Rev. **69**, 674 (1946).
[6] P. Tran, Phys. Rev. B **52**, 10673 (1995).
[7] V. Lousse and J. P. Vigneron, Phys. Rev. E **63**, 027602 (2001).
[8] *Nonlinear Photonic Crystals*, edited by R. E. Slusher, B. J. Eggleton, and Q.-G. J. Wang (Springer-Verlag, Berlin, 2003).
[9] M. Soljačić and J. D. Joannopoulos, Nature (London) **3**, 211 (2004).
[10] S. W. Leonard, H. M. van Driel, J. Schilling, and R. B. Wehrspohn, Phys. Rev. B **66**, 161102 (2002).
[11] D. A. Mazurenko, R. Kerst, J. I. Dijkhuis, A. V. Akimov, V. G. Golubev, D. A. Kurdyukov, A. B. Pevtsov, and A. V. Selkin, Phys. Rev. Lett. **91**, 213903 (2003).
[12] S. Barland *et al.*, Nature (London) **419**, 699 (2002).
[13] S. M. Spillane, T. J. Kippenberg, and K. J. Vahala, Nature (London) **415**, 621 (2002).
[14] F. Rossi and T. Kuhn, Rev. Mod. Phys. **74**, 895 (2002).
[15] J. Chen, H. A. Haus, S. Fan, P. R. Villeneuve, and J. D. Joannopoulos, J. Lightwave Technol. **14**, 2575 (1996).
[16] A. R. Jugessur, P. Pottier, and R. M. D. L. Rue, Electron. Lett. **39**, 367 (2003).
[17] J. Koga, Opt. Lett. **24**, 408 (1999).
[18] A. Taflove and S. C. Hagness, *Computational Electrodynamics: The Finite-Difference Time-Domain Method*, 2nd ed. (Artech House, Boston, 2000),
[19] R. W. Boyd, *Nonlinear Optics*, 2nd ed. (Academic Press, New York, 2002).
[20] We took $\epsilon_S=11.7045$, $\omega_0=1.1406\times10^{16}$, $\hat{\omega}_0=1.0995\times10^{15}$, $\gamma_0=3.802\times10^{8}$ (MKS units). Such values mimic the dispersion relation of $Al_{0.1}Ga_{0.9}As$.
[21] The value of $P_0^{-2}=3$ (MKS units) corresponds to $n_2=1.76\times10^{-17}$ W m^{-2}, as detemined by simulating self-phase modulation and evaluating n_2. The discretization steps are $dx=dy=dz=20$ nm, $dt\cong0.01$ fs.
[22] J. L. Young and R. O. Nelson, IEEE Antennas Propag. Mag. **43**, 61 (2001).
[23] R. W. Ziolkowski and E. Heyman, Phys. Rev. E **64**, 056625 (2001).
[24] A. Yariv and W. H. Louisell, IEEE J. Quantum Electron. **QE-2**, 418 (1966).
[25] H. A. Haus, *Waves and Fields in Optoelectronics* (Prentice-Hall, Englewood Cliffs, N.J., 1984).
[26] R. L. Shoemaker and F. A. Hopf, Phys. Rev. Lett. **33**, 1527 (1974).
[27] R. Loudon, *The Quantum Theory of Light*, 2nd ed. (Clarendon Press, Oxford, 1983).
[28] N. Bloembergen, Rev. Mod. Phys. **54**, 685 (1982).
[29] P. Meystre and M. Sargent III, *Elements of Quantum Optics* (Springer, Berlin, 1998).